Journal of Physical and Theoretical Chemistry
of Islamic Azad University of Iran, 9 (2) 117-123 summer 2012
(J. Phys. Theor. Chem. IAU Iran)
ISSN 1735-2126

Electronic Properties of Hydrogen Adsorption on the Silicon- Substituted C_{20} Fullerenes: A Density Functional Theory Calculations

F. R. Nikmaram[1,*] and Jamshid Najafpour[2]

[1]Department of Chemistry, Basic Science Faculty, Shahr-e-Rey Branch, Islamic Azad University, Tehran, Iran
[2] Department of Chemistry, Faculty of science, Science and Research Branch, Islamic Azad University, Tehran, Iran

Received December 2012; Accepted December 2012

ABSTRACT

The B3LYP/6-31++G** density functional calculations were used to obtain minimum geometries and interaction energies between the molecular hydrogen and nanostructures of fullerenes, C_{20} (cage), C_{20} (bowl), $C_{19}Si$ (bowl, penta), $C_{19}Si$ (bowl, hexa). The H_2 molecule is set as adsorbed in the distance of 3Å at vertical position from surface above the pentagonal and hexagonal sites of nanostructures. By comparing of gap energies, electronic chemical potential, hardness and results of QTAIM (Quantum Theory of Atom in Molecules) analysis, the Si atom substitution in hexa two-fold position of C_{20} (bowl) may be suitable for the adsorption of hydrogen molecule.

Keywords: C_{20} Fullerenes, Silicon substitution, Hydrogen Adsorption, NBO, QTAIM Analysis.

INTRODUCTION

Pure hydrogen may be the final destination in the evolution of fuel usage from coal to petroleum to natural gas, which has followed a trail of increasing hydrogen content [1]. A major bottleneck for the hydrogen vehicle is the problem of hydrogen storage. Jena describes the fundamental modes in which the H_2 molecule can be attached to a storage material [2]. He discusses the stringent requirements of the reversibility of the hydrogen uptake and release using each type of mechanism and emphasizes the use of nano sized configurations to improve the kinetics and thermodynamics of the candidate materials [2, 3]. Recently, considerable attention has been driven to porous materials such as zeolites, carbon nano tubes, and fullerenes as possible materials for hydrogen storage. C_{20} is regarded as the smallest experimentally synthesized carbon fullerene with 12 pentagons and bowl form of C_{20} with 6 hexagonal rings and a pentagon at center of structure [4]. Experimentally, each of these C_{20} isomers can be produced under suitable reaction conditions, For example, C_{20} fullerenes from its perhydrogenated form, dodecahedrane, $C_{20}H_{20}$ [5]. By comparing experimental photo-electron spectra with theoretical results, Saito and Miyamoto concluded that C_{20} fullerene should be a cage-type structure [6]. On the other hand, An et al, based on Hartree –

*Corresponding author: nikmaram88@iausr.ac.ir

Fock based CCSD (T) and MP4 results, concluded that bowl type structure would be the most stable structure [7, 8]. For C_{20} the most stable isomer can have a ring-shape, a bowl or a cage structure, depending on the computational method. Huda and co-workers found that bowl shaped C_{20} structure is more stable than the cage shaped [9]. The theoretical reports are available in the literature where carbon fullerenes were taken as base models for SiC fullerene structures. In Si substituted C_{20} clusters, the binding energies are higher for cage-type structure by almost 0.1 eV/atom over the bowl type structures [10, 11].

COMPUTATIONAL METHODS

In our study, the B3LYP/6-31++G** density functional calculations were used to obtain minimum geometries and interaction energies between the molecular hydrogen and nanostructures of fullerenes C_{20} (cage), C_{19} Si (cage), C_{20} (bowl), C_{19}Si (bowl, hexa two- fold) , C_{19}Si (bowl , hexa three- fold) and C_{19}Si (bowl, Penta) by Gaussian 03 package [12]. Then, H_2 molecule is adsorbed above the pentagonal and hexagonal sites. Using Natural Bond Orbitals (NBO) analysis, HOMO-LUMO gaps (HLG), electronic chemical potential, hardness and adsorption energies are obtained. A quantitative comparison of the bond strength can be given in terms of the bond topological properties. So, the wave functions obtained are evaluated with the program package AIMALL [13].

DISCUSSIONS

1. Geometry Optimization: In this research, the full optimization of geometries at B3LYP/6-31++G** method show that C_{20} cage (Fig.1) with -761.467 a.u. energy is more stable than C_{20} bowl (Fig.2) with -761.293 a.u. The Si substitution in both bowl and cage shape, of fullerene increase the stability. The Si substituted bowl structure at penta (Fig.3), hexa three- fold (Fig.4) and hexa two- fold (Fig. 5) positions are more stable than C_{19}Si cage (Fig.6) by 6.5676 a.u., 6.2909 a.u. and 6.648 a.u., respectively. The Si substitution at hexa two-fold position is more stable over the hexa three-fold by 0.358 a.u. in energy. The heteroatom substitution in the bowl fullerene may be suitable for the adsorption of hydrogen molecule. We study hydrogen molecule adsorption on all of structures. One hydrogen molecule is placed in the distance of 3 Å at vertical position from surface (Carbon or Silicon atom) in optimized configuration. One of the optimized structures of H_2 interaction with Fullerene is shown in Fig. 7. From our results, the effects of adsorption of H_2 on C_{19}Si (bowl, two- fold) at hexa position with 0.0814 a.u. and 0.358 a.u. change of the energy is stronger than C_{19}Si (bowl) at penta position and C_{19}Si (bowl, hexa three-fold), respectively. The adsorption energy, E_{ads}, is calculated using eq. (1). By definition, $E_{ads} < 0$ corresponds with more stablity and exothermic chemical bonding and $E_{ads}>0$ corresponds with endothermic chemical bonding. These energies show that the interaction between the H_2 molecule and C_{19}Si hexa, two- fold) is stronger than other interactions, Table 1.

2. NBO Analysis: The natural bond orbital (NBO) analysis were performed at the B3LYP/6-31++G** level using Gaussian 03. Using NBO analysis, HOMO-LUMO gaps, HLG (eq. (2)), electronic chemical potential (eq. (3)) and hardness (eq. (4)) are obtained [14].

The electronic chemical potential and hardness are defined as the following first-order [15, 16] and second-order [17, 18] derivatives, by (eq. (5)) and (eq. (6)) respectively.

$$E_{ads} = E_{(structure,\ H2)} - (E_{structure} + E_{H2}) \quad (1)$$

$$HLG = E_{LUMO} - E_{HOMO} \quad (2)$$

$$\mu = (E_{HOMO} + E_{LUMO})/2 \quad (3)$$
$$\eta = (E_{LUMO} - E_{HOMO}) / 2 \quad (4)$$
$$\mu = -\left(\frac{\partial E}{\partial n}\right) \quad (5)$$
$$\eta = 1/2(\partial^2 E/\partial N^2) \quad (6)$$

Table 1 presents the results of NBO analysis obtained by the DFT calculations. The energy gap between the highest occupied and the lowest unoccupied molecular orbitals (HOMO and LUMO, respectively), known as the HOMO–LUMO gap or simply HLG, is a critical parameter in determining molecular electrical transport properties,

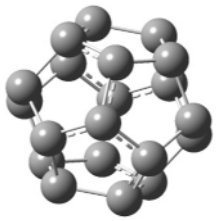

Fig. 1. C_{20} (cage).

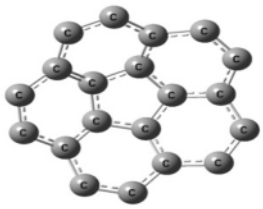

Fig. 2. C_{20} bowl.

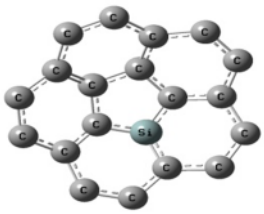

Fig. 3.$C_{19}Si$ (bowl, penta).

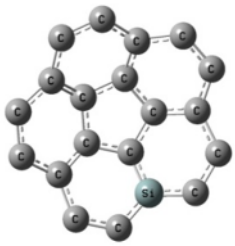

Fig. 4. $C_{19}Si$ (bowl , hexa, three- fold).

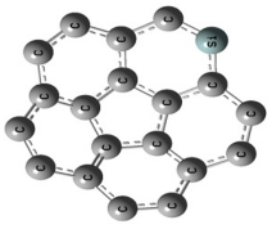

Fig. 5. $C_{19}Si$ (bowl, hexa, two- fold).

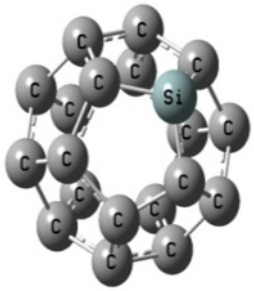

Fig. 6. $C_{19}Si$ cage.

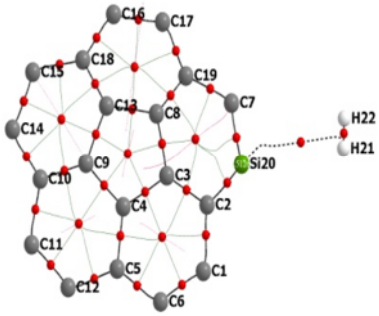

Fig. 7. H_2 interaction with $C_{19}Si$ (bowl, hexa, two-fold).

because it is a measure of electron conductivity. The energy gaps were determined by simply taking the differences in energy between HOMO and LUMO energy levels, (eq. (2)).

The gap energies of the bowl shapes decrease after adsorption, but these gaps increase for cage shapes. Since HLG is a measure of electrical conductivity, i.e. the decreasing trend in the HLG value means that electrical conductivity increases when the Hydrogen is adsorbed. After adsorption, the change of HLG ($HLG_{fullerene+H2} - HLG_{fullerene}$), change of

electronic chemical potential ($\mu_{fullerene+H2} - \mu_{fullerene}$), and change of hardness ($\eta_{fullerene+H2} - \eta_{fullerene}$), due to the polarization interaction between the charged Si atom and H_2 molecule at $C_{19}Si$ (hexa, two- fold) is stronger than other Hydrogen interactions. The gap energy of the $C_{19}Si$ (hexa, two- fold) after hydrogen adsorption, decreased from 88.621 kcal/mol to 81.462 kcal/mol, with ΔHLG equal to -7.159 kcal/mol. Therefore expected value of gap between valence and conduction band is shorter than other structures, so it indicates a maximum conduction in this structure.

Also the values for gap energy and hardness for all of the fullerene structures are smaller than the H_2 molecule (HLG for H_2 is 298.69 kcal/mol and η is 149.345 kcal/mol); these lead fullerene structures have higher polarizability than the H_2 molecule. Thus fullerene structures could accept electron from H_2. When hydrogen adsorbs on structures, electronic chemical potentials of $C_{19}Si$ (hexa, two- fold) will be decrease from -93.792 to -89.230 kcal/mol, with maximum of Δμ (4.518 kcal/mol), which is related to the highest stability of $C_{19}Si$ (hexa, two- fold), with H_2 system. The value of hardness for fullerene-H_2 is differing from the individual fullerene and H_2 molecule. The hardness of the $C_{19}Si$ (hexa, two- fold), with H_2 system was decreased (Δη = -3.5767 kcal/mol), this means that, the hardness of the fullerene is larger than the fullerene-H_2 system, and we can predict that the fullerene is relatively more stable and a physisorption process is dominant. So, in this system it shows, the H-H bond length expands slightly from 0.74252 Å to 0.74375 Å, (Table1).

3. AIM Analysis: The quantum theory of atoms in molecules (QTAIM) [19] (developed by Professor Richard F. W. Bader and his coworkers), relies on quantum observables such as the electron density ρ(r) and energy densities. A substantial aspect of Bader's theory of atoms in molecules (AIM; Bader, 1994) is the partitioning of a molecule into submolecular or even atomic regions [20, 21]. There is one BCP between each pair of atoms that are bonded, i.e., two atoms linked by a bond path and sharing a common interatomic zero-flux surface. In addition to the set of trajectories which terminate at the BCP and define an interatomic surface, a pair of trajectories originates at the BCP with each member of the pair terminating at one of the nuclei of the chemically bonded atoms. Chemical bonding interactions are characterized and classified according to the properties of the electron and energy densities at the BCP, collectively known as ''bond properties''. The Electron Density at the BCP (ρ_b) has been shown to be strongly correlated with the binding energy for several types of bonding interaction [22, 23]. Because the Laplacian is essentially a second derivative, its sign indicates regions of local electronic charge concentration or depletion with respect to the immediate neighborhood. Thus, where $\nabla^2\rho(r) > 0$ the density is locally depleted and expanded relative to its average distribution; where $\nabla^2\rho(r) < 0$ the density is locally concentrated, tightly bound, and compressed relative to its average distribution. The Laplacian of the electron density at the BCP ($\nabla^2\rho_b$) in covalent bonding is negative, $\nabla^2\rho_b < 0$. In contrast, in closed-shell bonding, for example ionic, hydrogen-bonding or van der Walls interactions, the interaction is characterized by a depletion of density in the region of contact of the two atoms and $\nabla^2\rho_b > 0$ [24]. A quantitative comparison of the covalent bond strength can be given in terms of the bond topological properties. Table 2 presents the results for the values of the charge density, the Laplacian at the

bond critical points, change of atom's charge (Δq) and change of kinetic energy of atom (Δk) obtained by the B3LYP/6-31++G** method. At all of the molecules the values of $\nabla^2\rho_b$ for adsorbent atom from fullerene structures and H from H_2 molecule at the adsorption site are positive, and that the bond character is physisorption with van der Walls interactions. The results obtained also showed large charge transfer from the H_2 to Si atom at the $C_{19}Si$ (hexa, two- fold), so that change of Si charge is -0.13132 a.u., and the most decrease of kinetic energy of Si at this system to predict a strong interaction of H_2 with $C_{19}Si$ (hexa, two-fold), (Fig.8).

Table 1. Energy of structures, adsorption energy, bond length, ΔHLG, μ & Δμ and η & Δη for systems.

Structure	E /a.u.	E_{ads} / kcal.mol^{-1}	[1]Bond length H-H /Å	ΔHLG/ kcal.mol^{-1}	μ/ kcal.mol^{-1}	Δμ/ kcal.mol^{-1}	η/ kcal.mol^{-1}	Δη / kcal.mol^{-1}
$C_{20\ cage}$	-761.4678	+0.313	-	0.0188	-105.125	-0.0627	21.805	0.00941
$C_{20\ cage}$,H_2	-762.6462		0.74336		-105.206		21.818	
$C_{19}Si_{\ cage}$	-1012.914	+0.564	-	1.7507	-94.457	0.6275	8.869	0.8753
$C_{19}Si_{\ cage}$,H_2	-1014.0920		0.74344		-93.290		9.745	
$C_{20\ bowl}$	-768.1884	-0.188	-	0.9977	-94.463	-0.4392	49.873	-0.4957
$C_{20\ bowl}$,H_2	-769.3490		0.74362		-94.903		49.377	
$C_{19}Si_{\ penta}$	-1019.4816	0.000	-	0.01255	-99.960	0.0502	33.201	-0.00627
$C_{19}Si_{\ penta}$,H_2	-1020.6605		0.74370		-99.910		33.194	
$C_{19}Si_{\ hexa,\ three-fold}$	-1019.2049	+0.062	-	0.8602	-95.208	0.6067	42.054	1.7204
$C_{19}Si$,H_2 $_{hexa,\ three-fold}$	-1020.3837		0.74369		-94.602		43.774	
$C_{19}Si_{\ hexa,\ two-fold}$	-1019.5619	-0.690	-	-7.1535	-93.792	4.518	44.307	-3.5767
$C_{19}Si$,H_2 $_{hexa,\ two-fold}$	-1020.7419		0.74375		-89.230		40.724	

Table 2. The Electron Density, Laplacian of the Electron Density at the BCP, (Δq) and Δk obtained by AIM analysis for systems.

structure	Connected atoms	ρ	$\nabla^2\rho$	[1]Δq	[2]Δk /a.u.
$C_{20\ cage}$, H_2	C_{16}-H_{21}	0.00341	+0.00956	C_{16}= 0.00836	C_{16}=0.0114
	H_{21}-H_{22}	0.26753	-1.3362		
C_{20} ,H_2 $_{bowl,\ penta}$	C_{14}-H_{31}	0.00006	+0.0002	C_{14}= -0.00062	C_{14}= -0.0014
	H_{31}-H_{32}	0.26717	-1.33484		
C_{20}, $H_{2\ bowl,\ hexa,\ two-fold}$	C_{18}-H_{32}	0.00176	+0.00548	C_{18}= -0.00112	C_{18}= -0.0040
	H_{31}-H_{32}	0.26749	-1.337745		
$C_{19}Si_{\ cage}$, H_2	Si_{20}-H_{22}	0.02642	+0.014	Si_{20}= -0.00332	Si_{20}= -0.0216
	H_{21}-H_{22}	0.26977	-1.47908		
$C_{19}Si$, H_2 $_{penta}$	Si_{30}-H_{31}	0.00723	+0.01824	Si_{30}= 0.02738	Si_{30}= -0.0080
	H_{31}-H_{32}	0.26891	-1.35104		
$C_{19}Si$, H_2 $_{heax,\ two-fold}$	Si_{30}-H_{31}	0.0071659	+0.0182	Si_{30}= -0.13132	Si_{30}= -1.2577
	H_{31}-H_{32}	0.265399	-1.30429		

[1]: $\Delta q = q_{\ atom\ after\ adsorption} - q_{\ atom\ before\ adsorption}$

[2]: $\Delta k = k_{\ atom\ after\ adsorption} - k_{\ atom\ before\ adsorption}$

CONCLUSIONS

In this research, we compared the effect of H_2 molecule adsorption on the electronic properties of the different structures of C_{20} (cage), C_{20} (bowl), $C_{19}Si$ (bowl, penta), $C_{19}Si$ (bowl, hexa three- fold) and $C_{19}Si$ (bowl, hexa two- fold) at the level of B3LYP/6-31++G** DFT calculations by Gaussian 03. Our results show that C_{20} (bowl), with H_2 system is more stable than the cage form by 6.7 a.u. in total energy. The ($C_{19}Si$ hexa two- fold, with H_2) system is more stable than (C_{20cage}, with H_2), ($C_{20,}$ $_{(}$bowl), with H_2) and (C_{19} Si (penta), with H_2) systems by 258.09, 251.39 and 0.1 a.u., respectively. In order to obtain the effects of the Hydrogen on the structures, NBO analysis was operated. By NBO analysis, HOMO-LUMO gaps, electronic chemical potential and hardness are obtained. NBO calculations essentially show significant change in the properties of $C_{19}Si$ (hexa two- fold) when H_2 molecule approach to this structure. In addition, the topological analysis of electronic density distribution in the theory of AIMs was used to compute some other molecular properties. The results of ΔHLG, $\Delta\mu$, $\Delta\eta$ and energy densities at the BCP indicate that hydrogen molecule binds molecularly to structures with a Van der walls interaction and Si atom substitution in hexa two- fold position provides suitable condition for hydrogen molecule adsorption.

REFERENCES

[1] L. Zhou,"Progress and Problems in Hydrogen Storage Methods Renewable Sustainable Energy" Rev.9 (2005) 395.

[2] P. Jena, "Materials for Hydrogen Storage: Past, Present, and Future", J. Phys. Chem. Lett 2 (2011) 206.

[3] J. Bisquert, J. Phys.Chem. Lett 2 (2011) 270.

[4] P. Pyykkö, C. Wang, M. Straka, J. Vaara, Phys. Chem. Chem. Phys 9(2007) 2954.

[5] Angew. Chem, Int.Ed 46 (2007) 742.

[6] M. Saito, Y. Miyamoto, Phys. Rev. B 65 (2002) 165434.

[7] W. An, Y. Gao, S. Bulusu, X.C. Zeng, J. Chem. Phys 122 (2005) 204109.

[8] C. Zhang, W. Sun, Z. Cao, J. Chem. Phys. 126 (2007) 144306.

[9] [A.K. Ray, M.N. Huda, J. Comput. Theor. Nanosci 3 (2006) 315.

[10] P. Melinon, B. Masenelli, F. Tournus, A. Perez, Nature Mater 6 (2007) 479.

[11] M.N. Huda, K. Ray, Chemical Physics Letters 457 (2008) 124.

[12] M. J. Frisch, G. W. Trucks, H. B. Schlegel, G. E. Scuseria, M. A. Robb, J. R. Cheeseman, J. A. Montgomery, Jr., T. Vreven, K.N. Kudin, J. C. Burant, J. M. Millam, S. S. Iyengar, J. Tomasi, O. Yazyev, A. J. Austin, R. Cammi, C. Dannenberg, V. G. Zakrzewski, S. Baboul, S. Clifford, J. Cioslowski, B.B. Stefanov, R.L. Martin, D.J. Fox, T. Keith, M.A. Al-Laham, C. Y. Peng, P. M. W. Gill, B. Johnson, W. Chen, M. W. Wong, C. Gonzalez, J.A. Pople, Revision B.03 ed., Gaussian, Inc., Pittsburgh PA,, 2003.

[13] F. Biegler-king, J. Schnbohm, D. Bayles, AIM 2000. A Program to Analyze and Visualize Atoms in Molecules, J. Comp. Chem 22 (2001) 545.

[14] J. P. Foster, J. Am. Chem Soc. 102 (1980) 7211.

[15] R. G. Pearson, Acc. Chem. Res. 26 (1993) 250.

[16] R. G. Pearson, R. A. Donnelly, M. Levy, W. E. Palke, J. Chem. Phys 68 (1978) 3801.

[17] R. G. Parr, R. G. Pearson, J. Am. Chem. Soc 105 (1983) 7512.

[18] A. Rafati, Journal of Colloid and Interface Science 336 (2009) 1.

[19] R. F. W. Bader, Atoms in Molecules: A Quantum Theory, Oxford University, Press: Oxford, U.K., 1990.

[20] R. F. W. Bader, H. Essen, J. Chem. Phys80 (1994) 1943.

[21] R. F. W. Bader, Can. J. Chem76 (1998) 973.

[22] M. Domagala, S. Grabowski, J. Phys. Chem. A 109 (2005) 5683.

[23] O. Knop, R. J. Boyd, S. C. Choi, J. Am. Chem. Soc. 110 (1988) 7299.
[24] C. F. Matta, R.J. Boyd, The Quantum Theory of Atoms in Molecules and Russell J. 2007 WILEY-VCH Verlag GmbH & Co. KGaA, Weinheim, page 11-16.